Journal of Global Positioning Systems (2006)
Vol. 5, No. 1-2:119-126

Journal of Global Positioning Systems
2006

Feasibility of Air Target Detection Using GPS as a Bistatic Radar

E. P. Glennon

SigNav Pty Ltd, Unit 2, 59 Tennant St, Fyshwick, ACT 2609, Australia

A. G. Dempster and C. Rizos

University of New South Wales, Sydney, NSW 2052, Australia

Abstract. The feasibility of using GPS as a bistatic radar illuminator for the purposes of air target detection is examined. The power budget analysis is first performed assuming the use of a single satellite, but is followed by a discussion of the expected improvements when multiple satellites are employed. The analysis includes the effect of GPS signal strength dynamic range, also known as the 'near-far' problem. The difference between the radar cross-section (RCS) of a typical air target and ground-based clutter reflections is discussed, followed by an estimation of the effect of ground clutter on the operation of such a system.

Keywords. Bistatic radar, Global Positioning System, radar detection,

1 Introduction

The Global Positioning System has found widespread application beyond standard positioning and timing, with new uses for GPS continually being developed. One of the more novel concepts is the secondary use of GPS signals for remote sensing, with the secondary application considered in this paper concerning the use of GPS satellite transmissions as the transmitter in a bistatic-radar for air target detection. Previous publications on this topic include (Tsui and Shaw, 1993) and (Koch and Westphal, 1995), although neither of those publications provides a power budget confirming the feasibility of the system. (Stolk and Brown, 2003) describes an airborne GPS remote sensing system capable of detecting large ocean vessels such as oil-tankers. Another paper by (Cherniakov et al., 2002) does provide a power budget estimate for air target detection, but assumes the use of the higher-powered IRIDIUM satellite system as the transmission source. Although the methodology of Cherniakov et-al (2002) has been adapted to the GPS case by (Mojarrabi et al., 2002), that analysis contained some errors. This paper duplicates the analysis of original Mojarrabi paper using a conventional approach and different parameter selections, resulting in less optimistic estimates for the maximum detection range.

The paper also estimates the effect of clutter in a GPS bistatic radar using a different technique to the methods of (Mojarrabi et al., 2002) and (Cherniakov et al., 2002). In addition, the effectiveness of using multiple GPS satellites on the power budget is also examined and difficulties due to the 'near-far' problem are discussed.

2 Bistatic GPS Power Budget

To determine the maximum range of a GPS-based bistatic radar it is necessary to determine the signal power that reaches the receiving antenna after being reflected from the target. For any radar, the power density of the target echo S_r at the receiver is given by (Skolnik, 1981):

$$S_r = \left(\frac{P_t G_t}{4\pi R_i^2} \right) \left(\frac{\sigma}{4\pi R_t^2} \right) \tag{1}$$

Here P_t is the transmitted power (W), G_t is the transmitter antenna gain (dimensionless factor), R_i is the range from the transmitter (satellite i) to the target (m), σ is the radar cross-section (RCS) of the target (m^2) and R_t is the range of the target from the receiver (m). The RCS is defined as the fictional area σ that produces the observed reflected power density S_r at a receiver at a range R from the target that has been illuminated with an incident power density of S_i (Skolnik, 1981).

$$\sigma = \lim_{R \to \infty} 4\pi R^2 \left(\frac{S_r}{S_i} \right) \tag{2}$$

The first term of the product in (1) is the power density of the direct (transmitted) signal at the target S_{direct} prior to being reflected (units of W/m^2).

The signal power available at the receiver antenna output depends on the effective area of the receiving antenna A_e, which depends on its gain:

$$A_e = \frac{\lambda^2 G_r}{4\pi} \tag{3}$$

where G_r is the receiver antenna gain and λ is the GPS carrier frequency wavelength of 0.19 m. Using (1) and (3) the power of the target reflection available at the receiver antenna output can be calculated as:

$$P_r = S_{direct}\left(\frac{\sigma}{4\pi R_t^2}\right)\left(\frac{\lambda^2 G_r}{4\pi}\right) \tag{4}$$

(4) permits the attenuation of the reflected signal measured using a high gain antenna relative to a standard directly received GPS signal as would be received in an omni-directional antenna with a gain of G_{0dBi} to be calculated:

$$\frac{P_r}{P_{direct}} = \left(\frac{\sigma}{4\pi R_t^2}\right)\left(\frac{G_r}{G_{0dBi}}\right) \tag{5}$$

To calculate the maximum range of such a system it is necessary to determine the noise level N_0 at the output of the RF front-end, which can be given in terms of the equivalent noise temperature T_{eff} and the bandwidth BW as:

$$N_0 = k\, T_{eff}\, BW \tag{6}$$

(4) and (6) allow the signal-to-noise ratio of the reflected signal at the RF front-end output to be written as:

$$\frac{P_r}{N_0} = \frac{S_{direct}\,\sigma\,\lambda^2\,G_r}{(4\pi)^2 R_t^2 \left(k\, T_{eff}\, BW\right)} \tag{7}$$

If the subsequent signal processing is then subject to losses L_{sp} and processing gain G_{sp} then the final signal to noise ratio ρ is given by:

$$\rho = \frac{S_{direct}\,\sigma\,\lambda^2\,G_r\,G_{sp}}{(4\pi)^2 R_t^2 \left(k\, T_{eff}\, BW\right) L_{sp}} \tag{8}$$

Assuming a minimum value for the detection signal-to-noise ratio permits an expression for the maximum range to be given as:

$$R_t = \sqrt{\frac{S_{direct}\,\sigma\,\lambda^2\,G_r\,G_{sp}}{(4\pi)^2 \rho_{\min} \left(k\, T_{eff}\, BW\right) L_{sp}}} \tag{9}$$

Using values for σ of 20 m^2, a horn antenna with a gain G_r of 15 dB (31.62) and a range R_t of say 10km, the reflected signal will be attenuated by about 62 dB, where this combination of parameters have been selected to agree with (Mojarrabi et al., 2002). Hence, if the direct signal has a signal-strength of say 52 dBHz or -152 dBW, then the reflection from the target will have a signal level of –10 dBHz or –215.2 dBW. Since the current state of the art in GPS receiver technology is to detect and track signals at around 20 dBHz, the detection of such a reflection is extremely difficult.

However, since such weak signal GPS receivers have typically been targeted for the E911 cellular application, some of the constraints present in the E911 case do not occur in the GPS bistatic radar application thereby permitting greater sensitivity to be achieved. In particular, since a bistatic GPS radar has simultaneous access to both the direct and indirect signals, the data received from the direct signal can be used to strip the data bits from the indirect signal, thereby permitting significantly longer coherent integration than the GPS data bit period of 20 ms. Appendix A (Van Diggelen, 2001) shows that for a coherent integration period of 1000 ms a maximum sensitivity of approximately -190 dBW or 13.2 dBHz is to be expected, assuming a final SNR of about 9.3 dB. This represents an attenuation of 38 dB compared to the typical maximum received signal of 52 dBHz, as is the case using a typical 3 dBi patch antenna. To calculate the range that this corresponds to, (4) can be used, setting P_r/P_{direct} to -38 dB (158.48×10^{-6}), G_{0dBi} to 3 dB (2), and using the previous values for σ and G_r, a value for R_t of 398m is obtained.

Table 1. Maximum Range Estimation Parameter Values

Parameter	Units	Values
S_{direct}	W/m^2	39.81×10^{-15}
S_{direct}	dBW/m^2	-134
σ	m^2	20
Bandwidth	Hz	2.4×10^{6}
T_{eff}	K	344
λ	m	0.19
G_{sp}	n/a	2.046×10^{6}
L_{sp}	n/a	2.11
G_r	n/a	31.62
k		1.38×10^{-23}
R_{max}	m	239

Alternatively, using (8) with the values given in Table 1 results in a maximum range of 239m. This value is lower than the previous value because it uses the minimum specified power spectral density for GPS of -134 dBW/m^2 (Spilker, 1996), whereas GPS satellites typically exceed the minimum level of performance. If the value for G_r is increased to 35 dBi (3481), which is equivalent to an antenna with effective area of

3.6m×3.6m (as used in (Cherniakov et al., 2002), then R_{max} increases to 2.51km.

3 Bistatic Radar / Multipath Paradox

The difficulty in detecting an air target reflection occurs because the power loss following reflection from the target is extremely high. This fact presents an apparent contradiction; which is how GPS multipath signals can ever be detected since in theory they should be significantly attenuated. The explanation is that there are essentially two types of reflections from a surface, namely specular reflections and diffuse reflections (Katzberg and Garrison, 1996). Multipath reflections are generally specular in nature, in which phase coherence is retained during the reflection process. However, reflections from an air target are generally diffuse reflections in which any incident radiation is scattered in multiple directions and phase coherence is lost.

This means that the RCS in the direction corresponding to a specular reflection is significantly greater than in the other directions, which are diffuse. This observation applies to both targets and clutter reflectors and is apparent on plots of RCS versus angle of incidence (Skolnik, 1981). Hence when a standard GPS receiver observes a multipath signal it generally corresponds to a specular reflection.

4 Clutter Power Estimate

The clutter power that is observed in a GPS bistatic radar system is dependent on the operating environment and the system characteristics. One factor under control of the designer is the receiving antenna. For this case, a suitable antenna is one in which there is high directivity and gain in a particular direction, but has small antenna sidelobes and gain in all other directions. The polarization of the antenna should be tuned to best match the polarization of the reflections and as such, will probably be left hand circular polarized (LHCP) which is opposite to the RHCP of the direct GPS signal. Clutter power is assumed to enter the system via the antenna sidelobes only, an assumption that is also made in (Cherniakov et al., 2002). The effect of observing the direct signal in the antenna main lobe is a more difficult issue that is separately considered in a subsequent section.

This analysis employs a simple antenna model in which the boresight gain G_r and beamwidth θ_{bw} are constant and the sidelobe gain G_{rsl} is constant and omni-directional. The model does not include realistically-shaped antenna sidelobes and is only intended for a first order analysis.

When calculating the clutter for a GPS bistatic radar, recall that GPS is a spread spectrum system with a chipping rate of f_c (1.023 MHz) and hence has a range resolution dR_c of c/f_c, where c is the speed of light. For this reason, the clutter will generally be range limited by the GPS range resolution of 293m. Assuming that all clutter is due to diffuse ground reflection, the power received at the antenna within a particular range cell R_t can be calculated as the power reflected by the area between the isorange contours on the ground starting at a range R_t and ending at $R+dR_c$ and adjusted for the free space loss of $1/(4\pi R_t^2)$. Using this procedure, the clutter power density at the receiving antenna can be given as

$$S_C = S_{direct}\,\frac{\sigma^0}{2}\log_e\left(1+\frac{dR_c}{R_t}\right) \tag{10}$$

where σ^0 is the RCS of the clutter per unit area and which is typically a function of the grazing angle, although for this analysis is taken to be constant. A derivation of this result is given in Appendix B.

The power of the clutter at the receiver antenna output can now be given as:

$$P_C = S_{direct}\,\frac{\sigma^0}{2}\log_e\left(1+\frac{dR_c}{R_t}\right)\left(\frac{G_{rsl}\,\lambda^2}{4\pi}\right) \tag{11}$$

This permits the clutter-to-target power ratio at the receiver antenna output to be given as:

$$\begin{aligned}\frac{P_C}{P_r} &= \frac{2\pi\sigma^0}{\sigma}\left(\frac{G_{rsl}}{G_r}\right)R_t^2\log_e\left(1+\frac{dR_c}{R_t}\right)\\ &\approx \frac{2\pi\sigma^0}{\sigma}\left(\frac{G_{rsl}}{G_r}\right)R_t\,dR_c\end{aligned} \tag{12}$$

Table 2. Clutter-to-Target Power Ratio

$\sigma^0(\alpha)$(dB)	G_{rsl} (dB)	R_t (m)	P_C/P_r (dB)
-20	0	1,000	-0.36
-20	-10	1,000	-10.36
-20	-10	5,000	-3.37
-20	-10	10,000	-0.36
-2	-10	1,000	7.64
-2	0	1,000	17.64

Table 2 gives the clutter-to-target power ratio for various values of σ^0, R_t and G_{rsl}. The σ^0 values of -20 dB and -2 dB are taken from (Willis, 1995) and correspond to data for "out-of-plane, horizontally polarized, σ_B^0 data for tall weeds and scrub trees" measured at a frequency of 1.3 GHz, a value that is close to the GPS carrier frequency of 1.57542 GHz. The maximum value for this parameter is about -2 dB corresponding to a specular reflection, while the typical value is about -20 dB. The minimum value is about -30 dB. All data is for bistatic mode of operation. The sidelobe gain values for G_{rsl} are

estimates only. Values for G_r and σ have been chosen as 30 dB and 20 m^2 respectively to match the previous section and dR_c has been set at 293m.

This data shows that even for relatively short ranges, the clutter contains almost as much power as the target radar return. The situation can be improved by reducing the magnitude of the antenna sidelobe gain. However, occasionally it will be possible that 'specular' type clutter will occur that will completely dominate over the target reflection.

One factor that has not been taken into account is the clutter Doppler frequency, where the analysis assumes that the clutter will have the same Doppler offset as the target. This is not realistic for air targets thereby enabling the option of using Moving Target Indicator (MTI) to separate the target from the clutter. The use of MTI is consistent with the use of long coherent integration and its associated narrow bandwidths required for the detection of very weak signals. Proper analysis of the MTI improvement is beyond the scope of this paper and in the case of GPS, care must be taken since the Doppler frequency return varies with distance from the receiver.

5 GPS 'Near-Far' Problem

Cross-correlation or the 'near-far' problem occurs when trying to detect weak GPS signals in the presence of other strong GPS signals. Due to the use of 10-bit Gold codes, the dynamic range of the GPS C/A code is normally limited to signal levels that are no more than 21.6 dB weaker than the strongest signal present (Spilker, 1996).

Since the target signal reflections that need to be detected by a GPS-based bistatic-radar are significantly weaker than the strongest signals present, this presents a clear limitation that must be addressed. There are several methods that could be used to suppress the strong GPS signals. One method is to employ a highly directional high-gain antenna that has very low-gain sidelobes, although this will probably result in the strong signal suppression of between 30 to 40 dB, assuming the antenna gain is about 30 to 40 dB above the sidelobes. However, it has already been shown that target echoes could easily be attenuated by approximately 60 dB compared to the main signal, so unless additional cross-correlation mitigation techniques are employed reliable detection of the reflections is unlikely. Such techniques range from cancellation to subspace projection techniques (Madhani et al., 2003; Glennon and Dempster, 2004; Glennon and Dempster, 2005), although no commercial-off-the-shelf GPS chipsets currently implement cross-correlation mitigation therefore leaving software correlation as the only viable alternative. Cross-correlation mitigation represents a challenging problem and has applications for weak signal GPS receivers in general, although since these techniques are not in widespread use it is difficult to estimate their effectiveness.

One interesting case that can arise is when the target happens to lie in the line-of-sight of a GPS satellite. Clearly the receiving antenna offers no protection against cross-correlation since the both reflection and direct signal are amplified equally. However, from a bistatic radar point of view this case is significant for another reason, namely the forward scatter RCS of the target experiences significant enhancement compared to the typical value. The forward-scatter RCS σ_F for a target is given by (Willis, 1995):

$$\sigma_F = \frac{4\pi A^2}{\lambda^2} \tag{13}$$

where A is the target shadow area. If (13) is substituted into (4), then the power reflected by the target and received by the receiver can be expressed as:

$$P_r = S_{direct} \left(\frac{1}{4\pi\ R_t^2} \right) A^2\ G_r \tag{14}$$

Assuming that the direct signal is not significantly attenuated due to blockage by the target, then the direct received signal power at the antenna output is:

$$P_{direct} = S_{direct} \left(\frac{\lambda^2\ G_r}{4\pi} \right) \tag{15}$$

and the ratio of the reflected to the direct signal is:

$$\frac{P_r}{P_{direct}} = \frac{A^2}{R_t^2\ \lambda^2} \tag{16}$$

It should also be noted that according to (Koch and Westphal, 1995) this assumption about the direct signal not being attenuated may not be entirely true. This is because the target size could be comparable to the size of the first Fresnel zone, this being the size at which significant RF blockage becomes apparent. If this is the case then it means that better results than the above analysis predicts may be expected.

The other difficulty with this particular scenario is that the path difference between the direct path and the reflection will be smaller and unless it exceeds one GPS chip (293m), separation of the two signals will be difficult. The geometry of this scenario also means that the velocity of the target cannot be determined since the Doppler difference between the direct and indirect path is small.

Using a value for A of 5 m^2 and a value for R_t of say 10km, the attenuation of the reflection compared to the direct signal comes out at about 51.6 dB. As a result, although the forward scatter enhancement of the RCS is

quite significant (σ_F/σ is 26 dB), the benefit is partially cancelled by the loss of the antenna directivity and gain in reducing the direct signal.

This analysis shows that the forward scatter RCS enhancement advantage may not be as beneficial as expected and is still very much dependent on the properties of the receiving antenna system. This is because the forward scatter RCS effect typically takes place when the bistatic angle is within 10° of the 180° ideal angle. This means that for an extremely narrow antenna beam-width it would still be possible to gain some of the advantage of the enhanced RCS while still gaining the benefit of some reduction in the direct signal. However trying to analyze a case such as this using the simple antenna model employed in this paper clearly represents a limitation of this approach, with a proper analysis of this particular case requiring a particular antenna and target RCS profile be employed.

The GPS front-end chip may also fail to operate correctly if the input signal levels exceed its design parameters.

6 Use of Multiple Satellites

Up to this point the analysis has assumed the use of a single GPS satellite and a single GPS receiver. However, the number of visible satellites varies from a minimum of about four to a maximum of about twelve satellites and this presents an opportunity to improve performance.

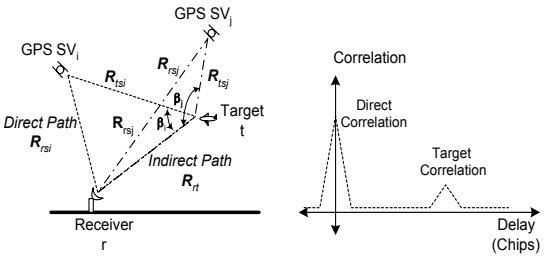

Fig. 1. System Geometry & Correlation Curves

Figure 1 shows the system geometry for a GPS bistatic radar as well as an illustration of one of the correlations that could be expected (neither to scale). The difficulty in using multiple satellites arises because although the range from the target to the receiver is the same for all satellites, the multipath delay between the direct path and the reflected path is not. For the example, the multipath delay for SV_i would be expected to be larger than for SV_j which is closer to the line-of- sight (LOS).

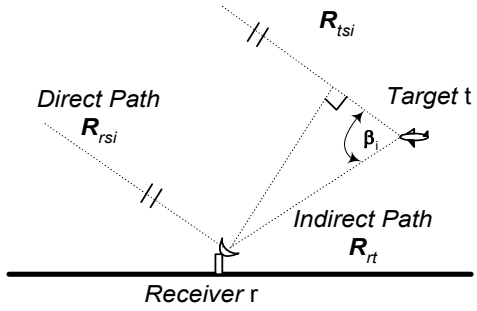

Fig. 2 Delay Path Length

If the range vectors from the receiver to satellite *i*, the target to satellite *i* and the receiver to the target are denoted by $\mathbf{R}_{rsi}$, $\mathbf{R}_{tsi}$ and $\mathbf{R}_{rt}$ respectively and the bistatic angle is given by β_i, then the multipath delay $c\Delta t$ between the direct path and the reflected path is given by:

$$\begin{aligned} c\,\Delta t &= d_1 + \left\|\mathbf{R}_{rt}\right\| \\ &= \left\|\mathbf{R}_{tsi}\right\| - \left\|\mathbf{R}_{rsi}\right\| + \left\|\mathbf{R}_{rt}\right\| \\ &= \left\|\mathbf{R}_{rt}\right\| \cdot \cos(\beta_i) + \left\|\mathbf{R}_{rt}\right\| \\ &= 2 \cdot \left\|\mathbf{R}_{rt}\right\| \cdot \cos^2(\beta_i/2) \end{aligned} \tag{17}$$

(17) makes it possible to predict the multipath delay for a given target range and bistatic angle (the angle between the transmitter and receiver measured at the target). Since the range from the target to the receiver is fixed across all satellites and the bistatic angle is constant for a given satellite on a particular target LOS vector, it is possible to scale the correlation outputs for each satellite so that the target delays are the same for all satellites. Provided this is done after removal of the direct signal (to remove the effect of local correlation peaks and cross-correlations), it should be possible to accumulate the scaled correlation outputs from all satellites together.

The most straightforward method of accumulating correlations across multiple satellites is to do so non-coherently by first taking magnitudes of the complex correlation outputs. The improvement that is to be expected can be approximated by assuming that use of N_{sv} satellites each with power spectral density S_{direct} is equivalent to the use of a single satellite with power spectral density $N_{sv} \times S_{direct}$. Unfortunately this approach suffers from the problem of non-linear integration loss (Barton, 1969; Lin et al., 2002), where the magnitude of the loss depends on the signal detectability-factor (signal-to-noise ratio) as well as the number of non-coherent integrations performed. A plot of integration loss versus number of integrations for different output single-pulse detectability factors $D_0(1)$ can be found in (Barton, 1969) and is reproduced below in Figure 3.

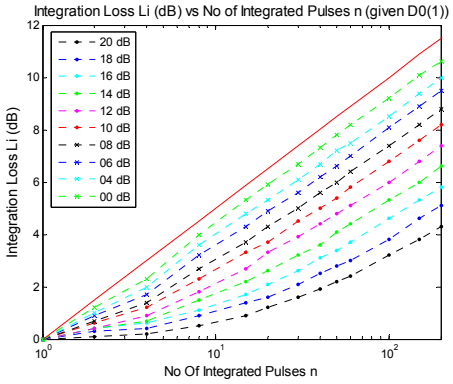

Fig 3. Non-coherent integration loss for a given number of integration periods.

To obtain the integration loss L_i, the detectability factor $D_0(1)$ that provides required probability of false-alarm P_{fa} and probability of detection P_d for a single pulse detector is determined using Rayleigh-Rice probability distribution curves. The loss caused by obtaining this quantity through integration of multiple pulses can then be determined by interpolating the curves given in Figure 4 for the given value of $D_0(1)$ and then reading the loss corresponding to the number of non-coherent integrations n. For the multiple GPS satellite case, the value of n will range from between 4 and 12, while for a P_{fa} of less than 10^{-6} and a P_d of greater than 0.9 a $D_0(1)$ value of greater then 13 dB is required (Barton, 1969). These combinations of parameters imply an integration loss of less than 2 dB.

Depending on the signal strength of the target reflection, this accumulation across multiple satellites should result in improved detectability. More importantly however, with the use of multiple satellites the bistatic angle for one of the satellites may be more favourable, leading to a better RCS, also improving the probability of detection.

It is probably not possible to perform a fully coherent integration across multiple satellites since the phase coherence of the signal is unlikely to be retained during the diffuse reflection process. As a result, the integration losses of the non-coherent process probably cannot be eliminated.

7 Conclusions

This analysis has shown that due to the extreme weakness of the transmitted GPS signal, detection of targets with small RCS using receive antennas of gain 15 dB is probably not feasible. Other problems that need to be overcome involve the 'near-far' problem caused by the dynamic range of the received GPS signals and the problem of the received ground clutter power having a greater power level than the target reflection. Given these difficulties, the following recommendations are suggested if construction of such a system is to be undertaken.

Firstly, the gain of the receive antenna should be as large as possible. The worked example used a horn antenna with a gain of 15 dB, however it should be possible to achieve a gain of say 25 dB which would increase the maximum range by a factor of 3. Secondly extremely long coherent integration periods of approximately 1 to 2 seconds using full data-wiping should be employed. Thirdly, the method of non-coherently combining the output from all the available satellites should be implemented. Since there are generally at least 6 satellites visible and sometimes as many as 12, this would probably increase the maximum range by a further factor of 1.5 to 3, depending on the squaring loss. GPS signal cancellation techniques need to be developed in order of mitigate against the 'near-far' problem.

Use of the system could also be limited to detection of larger targets (with larger RCS) thereby also increasing the detection range, although if a sufficient number of satellites are present then some may have a more favourable geometry than others resulting in a better RCS in these circumstances.

In conclusion, it has been shown that implementing a GPS-based bistatic radar for the purposes of target detection is significantly constrained by the available power budget. These constraints explain why the patent (Tsui and Shaw, 1993) and early-published papers (Koch and Westphal, 1995) do not appear to have resulted in any follow-on work. However, it is possible that use of the suggestions outlined above and the availability and use of new GNSS signals could permit construction of a workable system, albeit one with limited maximum range.

Appendix A: Maximum GPS Sensitivity

To estimate the maximum sensitivity of a GPS receiver it is first necessary to estimate the noise figure of the RF front-end (Figure 4) using the Friss formula (Van Dierendonck, 1996). Table 3 shows the resulting noise figure and effective temperature at each stage of the process with typical values for the gain, loss and noise figures. The end result is a total noise figure NF_T of 2.4 dB and effective temperature T_{eff} of 344 K assuming an antenna source temperature T_A of 130 K.

Using the effective temperature of the front-end (FE) and assuming availability of the full GPS navigation message to enable data wiping on the detected signal and hence enabling long coherent integration, the ability to detect various signal levels can be established. Table 4 (Van Diggelen, 2001) shows that with a very weak input signal of -160 dBm at the antenna output and using a 1 second

coherent integration period with full data wipe, the output signal to noise ratio is 9.3 dB and therefore at the limit of detectability.

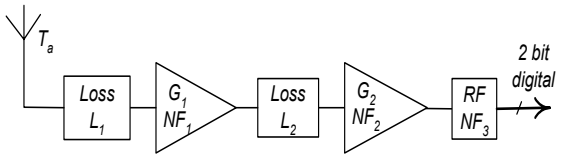

Fig. 4 RF Front-End

Table 3. Front-End Noise Figure

	L1	G1	L2a	L2b	G2	FE
Gain (dB)	0.10	19.0	6.0	3.00	19.0	
Gain	0.98	79.4	0.3	0.50	79.4	
Total Gain	0.98	77.6	19.5	9.8	776	
NF (dB)	0.10	1.9	6.0	3.0	1.9	9.0
$F = 10^{NF\,(db)\,/\,10}$	1.02	1.6	4.0	2.0	1.6	7.9
Total F_T	1.02	1.6	1.6	1.7	1.7	1.7
Total NF_T (dB)	0.10	2.0	2.1	2.3	2.4	2.4
$T_{eff}=T_A+(F_T-1)\,T_0$	137	300	311	326	342	344

Table 4. Maximum GPS Sensitivity

Parameter	Value	Notes
Antenna OP (dBm)	-160.0	Signal at Antenna Output
Antenna OP (dBHz)	13.23	AntOP–30+10 $\log_{10}(kT_{eff})$
IF Bandwidth (MHz)	2.40	Typical RF FE is 2.4 MHz within 3dB.
T_{eff} (K)	344.40	FE effective temperature
Noise power (dBm)	-109.43	10 $\log_{10}$ ($k\,T_{eff}\,BW$) + 30
IF SNR (dB)	-50.57	Ant OP - Noise power
Input Bandwidth (MHz)	2.046	
Coherent Period (ms)	1000.0	Coherent integration
Output Bandwidth (Hz)	1.00	1/Coherent Integration
Coherent Gain	1430.4	√(Input BW/Output BW)
Coherent Gain (dB)	63.1	20 $\log_{10}$(Coherent Gain).
Mistuning Loss (dB)	2.0	Correlation&Mistuning loss
Quantization Loss (dB)	1.25	2-bit quantization Loss
Actual Gain (dB)	59.9	Coherent Gain – Losses
Final SNR (dB)	9.3	IF SNR + Actual Gain
Final SNR (ratio)	2.91	Peak/sigma ratio = $10^{(dB/20)}$

Appendix B: Clutter Power Density Estimation

The clutter power density affecting a target at range $\mathbf{R}_t$ can be estimated by integrating the power reflected from the ground between the isorange contours, starting from R_t and ending at R_t+dR_c with a free-space loss-factor weighting of $1/(4\pi R_t^2)$. This isorange contour can be obtained for a given multipath delay $c\Delta t$ using the relationship (Stolk and Brown, 2003)

$$\begin{aligned} c\Delta t &= \left\| \mathbf{R_{rt}} \right\| - \mathbf{R_{rt}} \cdot \mathbf{k_i} \\ &= \left\| \mathbf{R_{rt}} \right\| + \left\| \mathbf{R_{rt}} \right\| \cos\beta_i \end{aligned}$$

where $\mathbf{R}_{rt}$ is the range vector from the receiver to the target (clutter) , $\mathbf{k}_i$ is the unit line-of-sight vector to the satellite and β_i is the (bistatic) angle between $\mathbf{R}_{rt}$ and $\mathbf{k}_i$. Assuming a flat earth model with the receiver at the origin, the multipath delay can be written as:

$$\begin{aligned} \mathbf{k_i} &= \begin{pmatrix} \cos(e)\cos(a) & \cos(e)\sin(a) & \sin(e) \end{pmatrix} \\ \mathbf{R_{rt}} &= \begin{pmatrix} R_c\cos\theta & R_c\sin\theta & 0 \end{pmatrix} \\ &= \begin{pmatrix} x & y & 0 \end{pmatrix} \\ c\Delta t &= R_c - R_c\cos\theta\cos(e)\cos(a) - R_c\sin\theta\cos(e)\sin(a) \\ &= R_c\left(1-\cos(e)\cos(\theta-a)\right) = R_t \end{aligned}$$

where e is the satellite elevation, a is the satellite azimuth and R_c and θ are the range and angle from the receiving antenna to the clutter respectively. Hence the isorange clutter contour $Iso(R_t)$ for a target at a range R_t occurs at a clutter range R_c is defined by:

$$R_c = Iso\left(R_t\right) = R_t / \left(1-\cos(e)\cos(\theta-a)\right)$$

A clutter element at $\mathbf{R}_{rt}$ contributes dS_C to the total clutter power density, where σ^0 is the clutter RCS per unit area.

$$dS_C = \frac{S_{direct}\ \sigma^0}{4\pi R_c^2} R_c\, dR_c\, d\theta$$

Applying a change of variables from clutter range to target range and then integrating dS_c over the full θ range and a target range with the applicable range resolution yields the total clutter power density as required:

$$\begin{aligned} S_C &= \int_0^{2\pi} \int_{Iso(R_{t0})}^{Iso(R_{t0}+dR_c)} \frac{S_{direct}\,\sigma^0}{4\pi R_c^2} R_c\, dR_c\, d\theta \\ &= \frac{S_{direct}\,\sigma^0}{4\pi} \int_0^{2\pi} \int_{R_{t0}}^{R_{t0}+dR_c} \frac{\left(1-\cos(e)\cos(\theta-a)\right)dR_t}{\left(1-\cos(e)\cos(\theta-a)\right)R_t} d\theta \\ &= \frac{S_{direct}\,\sigma^0}{4\pi} \int_0^{2\pi} d\theta \int_{R_{t0}}^{R_{t0}+dR_c} \frac{dR_t}{R_t} \\ &= \frac{S_{direct}\,\sigma^0}{2} \log\left(1+\frac{dR_c}{R_{t0}}\right) \end{aligned}$$

Note that the total clutter power density is independent of satellite position despite the fact that this is not the case for the isorange contours. A cross check for the case where the bistatic illuminator is directly overhead can be performed since in this case the isorange contours are

concentric circles around the antenna, yielding approximation (12).

Acknowledgement

This research was supported by the Australian Research Council Discovery Project DP0556848. Comments by Rod Bryant on the use of multiple satellites are also gratefully acknowledged.

References

Barton D. K. (1969) ***Simple Procedures for Radar Detection Calculation***. IEEE Trans. AES-5, Vol. 5, pp. 837 - 846.

Cherniakov M., Nezlin D. and Kubik K. (2002) ***Air target detection via bistatic radar based on LEOs communication signals***. Radar, Sonar and Navigation, IEE Proceedings -, Vol. 149(1), pp. 33-38.

Glennon, E.P. and Dempster A.G. (2004) ***A Review of GPS Cross Correlation Mitigation Techniques***. The 2004 International Symposium on GNSS/GPS, Sydney, Australia, 6 - 8 December 2004.

Glennon E. P. and Dempster A. G. (2005) ***A Novel GPS Cross Correlation Mitigation Technique***. ION GNSS 2005, Long Beach, CA, 13 September 2005.

Katzberg S.J. and Garrison J.L. (1996) ***Utilizing GPS to Determine Ionospheric Delay Over the Ocean***, NASA.

Koch V. and Westphal R. (1995) ***New approach to a multistatic passive radar sensor for air/space defence***. Aerospace and Electronic Systems Magazine, IEEE, Vol. 10(11), pp. 24-32.

Lin D.M., Tsui J.B.Y., Liou L.L. and Norton Y.T.J. (2002) ***Sensitivity Limit of a Standalone GPS Receiver and an Acquisition Method***. ION GPS 2002, Portland, OR, 24-27 September 2002.

Madhani P.H., Axelrad P., Krumvieda K. and Thomas J. (2003) ***Application of successive interference cancellation to the GPS pseudolite near-far problem. Aerospace and Electronic Systems***, IEEE Transactions on, Vol. 39(2), pp. 481-488.

Mojarrabi B., Homer J., Kubik K. and Longstaff I.D. (2002) ***Power budget study for passive target detection and imaging using secondary applications of GPS signals in bistatic radar systems***. Geoscience and Remote Sensing Symposium, 2002. IGARSS '02. 2002 IEEE International,pp. 449-451.

Skolnik M.I. (1981) ***Introduction to Radar Systems: Second Edition***, McGraw-Hill.

Spilker J.J. (1996) ***Signal Structure and Theoretical Performance***. Global Positioning System: Theory and Applications Volume 1. B. W. Parkinson, J. J. Spilker, P. Axelrad and P. Enge, American Institute for Aeronautics and Astronautics,Vol. 163, pp. 57 - 119.

Stolk K. and Brown A. (2003) ***Bistatic Sensing with Reflected GPS Signals Observed With a Digital Beam Steered Antenna Array***. ION GPS 2003, September 2003.

Tsui J.B.Y. and Shaw R.L. (1993) ***Passive Ranging Through Global Positioning System***, United States of America Patent 5,187,485

Van Dierendonck A.J. (1996) ***GPS Receivers***. Global Positioning System: Theory and Applications Volume 1. B. W. Parkinson, J. J. Spilker, P. Axelrad and P. Enge, American Institute for Aeronautics and Astronautics,Vol., pp. 329 - 407.

van Diggelen F. (2001) ***Course 240A: Indoor GPS I***, Salt Lake City, Utah, 11 September 2001.

Willis N.J. (1995) ***Bistatic Radar: 2nd Edition***, Technology Service Corporation.